

Factors affecting web-shear capacity of deep hollow-core units

Keith D. Palmer
and Arturo E. Schultz

Precast, prestressed concrete hollow-core units are plant-fabricated members with continuous voids cast on beds ranging from 300 ft to 600 ft (90 m to 180 m) in length. **Figure 1** shows the cross section of three hollow-core units, the top one with circular voids and the bottom two with noncircular voids. The continuous voids reduce the amount of concrete used, thereby decreasing the unit's weight and providing space for concealed electrical or mechanical chases. The concrete displaced by the voids does

Editor's quick points

- Recent shear tests by several U.S. manufacturers on thick hollow-core units have indicated shear failures in the web at forces smaller than those predicted by *Building Code Requirements for Structural Concrete (ACI 318-05) and Commentary (ACI 318R-05)*.
- This paper highlights the main parameters affecting the web-shear capacities of hollow-core units as demonstrated by previous and current research.
- The web-shear capacities of hollow-core units produced by two U.S. manufacturers are compared using ACI 318-05, *Eurocode No. 2: Design of Concrete Structures-Part 1: General Rules and Rules for Buildings*, the modified compression field theory, the American Association of State and Highway Transportation Officials' *AASHTO LRFD Bridge Design Specifications*, and Yang's method.

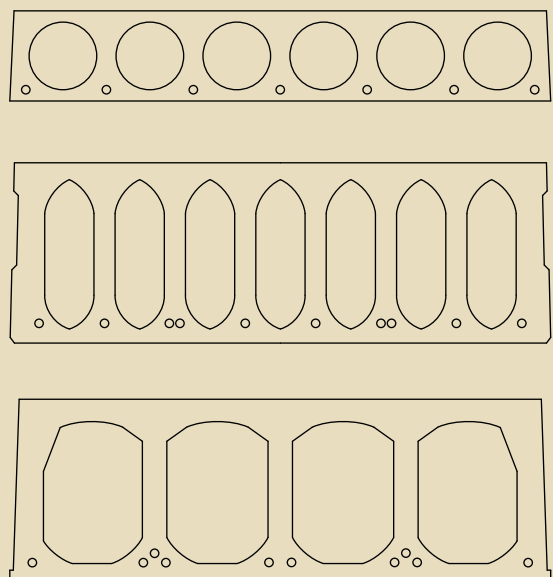


Figure 1. The continuous voids of these hollow-core-unit cross sections reduce the amount of concrete used, thereby decreasing unit weight and providing space for concealed electrical or mechanical chases.

not contribute significantly to flexural capacity, thereby justifying these complex cross sections. Hollow-core units are typically reinforced with longitudinal prestressing strands only. Longitudinal mild-steel reinforcement is typically not necessary, and the manufacturing process restricts the use of shear reinforcement such as stirrups. Hollow-core units are primarily used as floor and roof framing but are also used as wall and spandrel members.

Hollow-core units are typically manufactured using one of two methods.¹ The first is the extrusion method, which forces a dry, low-slump concrete through an extrusion machine that forms the cores with augers or tubes. The second method uses a higher-slump concrete that is fed into the casting machine; the sides are formed with stationary forms or slip forms that move with the machine. The casting methods and equipment are proprietary, and there are about eight major manufacturers of hollow-core-unit equipment in the United States.²

The depths of hollow-core units in the United States have historically been limited to 8 in., 10 in., and 12 in. (200 mm, 250 mm, and 300 mm). Depths of up to 20 in. (510 mm) are widely used in Europe and are gaining popularity in the United States because of improved manufacturing technology and their ability to sustain higher loads and span longer lengths than the shallower sections.

In the United States, the design of hollow-core units is governed by the American Concrete Institute's (ACI's) *Building Code Requirements for Structural Concrete (ACI 318-08) and Commentary (ACI 318R-08)*.³ Design guidance can also be found in the *PCI Manual for the Design of Hollow Core Slabs*.¹

Impetus for research

The shear behavior of concrete has been studied for more than 100 years, and there is still no universally accepted method for shear design. The shear behavior of a concrete member cannot be understood from an approach as basic as that used for flexure. Most equations predicting the shear capacity of concrete members are derived empirically, and they vary depending on the type and configuration of loading and the type of reinforcement (unreinforced, reinforced, and/or prestressed). In addition, it has been shown that the member size can influence the strength of the member in shear, particularly for members without shear reinforcement.⁴⁻⁷ As the depth of the member increases, the shear stress at failure decreases. This phenomenon is known as the size effect in shear.

Due to the size effect and the sudden and brittle nature of shear failures, ACI 318-08 requires a minimum amount of shear reinforcement in concrete members. However, this requirement was waived for slabs, including hollow-core units, and footings by ACI 318-05⁸ due to the reduced

probability of overloading a wide member as well as the potential for load redistribution in ductile flexural members. Concerns have been raised that thicker hollow-core units (that is, ones with depths greater than 12 in. [300 mm]) may fail in shear at lower loads than those predicted by ACI 318-05. In fact, recent tests² of hollow-core units by several U.S. manufacturers have shown that this is indeed the case, with some of the tested units failing in web shear at 60% or less of the load predicted by ACI 318-05. This lower capacity based on traditional web-shear-design methods agrees with the European experience with thicker hollow-core units.^{9,10} As a consequence, ACI 318-08 now requires minimum shear reinforcement to be supplied in hollow-core units with depths greater than 12.5 in. (318 mm) if the factored shear force exceeds 50% of the design shear strength of the concrete. Otherwise, the web-shear capacity must be reduced by 50%.

Research objectives

An analytical research program was undertaken at the University of Minnesota to better predict the web-shear capacities of thick hollow-core units and to quantify the reasons that these thicker units are failing at lower shears than those predicted by ACI 318-05. This paper highlights the main parameters affecting the web-shear capacity of hollow-core units as demonstrated by previous and current research. In addition, the results of recent tests by two U.S. manufacturers will be compared using a number of shear prediction methods. These methods include ACI 318-05,⁸ *Eurocode No. 2: Design of Concrete Structures-Part 1: General Rules and Rules for Buildings*,¹¹ the modified compression field theory,^{12,13} the American Association of State and Highway Transportation Officials' (AASHTO's) *LRFD Bridge Design Specifications*,¹⁴ and Yang's method.¹⁰ Comments are also made regarding the effect of the change made in ACI 318-08.

Shear design

Section 11.4.3 of ACI 318-08 and ACI 318-05 explicitly recognize two different types of shear failure: web-shear failure and flexure-shear failure. A web-shear failure is defined as a failure that occurs when the principal tensile stress in the web near the support of a member, which is uncracked in bending, reaches the limiting tensile strength of the concrete typically along an inclined path. A flexure-shear failure typically occurs farther away from the support, where the flexural stresses are high enough to cause vertical cracks to form and the shear stresses have not diminished enough to be negligible. A vertical flexural crack forms first and becomes inclined when the shear stress at the crack tip is large enough to cause an inclination of the crack. The ACI 318-05 expression for the web-shear failure mode is based on a mechanics-of-materials approach, while the flexure-shear expression is empirical. This paper deals only with the web-shear failure mechanism because

the recent tests by U.S. manufacturers² (denoted as supplier A and supplier B in this paper) showed that none of the hollow-core units exhibited flexure-shear capacities that were lower than those predicted by ACI 318-05.

Parameters affecting web-shear capacity of hollow-core units

There are a number of parameters that may affect the web-shear capacity of hollow-core units. Some of these parameters are considered in the ACI 318-08 and ACI 318-05 formulation, while a number of them are not. These parameters include the following:

- overall thickness or height of the member h
- geometry of the cross section, including cross-section properties, such as gross area of concrete A_g , moment of inertia I , first area moment of section Q , web width b_w , and distance from extreme compression fiber to centroid of prestressing steel d_p
- compressive stress in concrete at centroid of cross section resisting externally applied loads after allowance for all prestress losses f_{pc} , which is a function of effective stress in prestressing steel after allowance for all prestress losses f_{se} and A_g , and its development into the section
- tensile strength of the web concrete f_{ct}
- variation of (that is, shear lag of) prestressing force throughout the depth and across the width of the unit
- shear span-to-depth ratio a/d_p

Of the listed parameters, ACI 318-08 and ACI 318-05 consider b_w , d_p , f_{pc} , the development of prestressing force

into the section, and f_{ct} of hollow-core units. The following sections will describe each parameter and its possible effect on the shear capacity of hollow-core units.

Depth of the member

A number of researchers⁴⁻⁷ have shown that for members without transverse reinforcement or distributed longitudinal reinforcement throughout the depth, the average shear stress at failure tends to decrease as the depth of the member increases. This is the size effect in shear. Angelakos et al.⁷ showed that this phenomenon becomes important or critical at depths greater than about 20 in. (510 mm) for rectangular sections. Collins and Kuchma⁵ suggested that the size effect is more a function of the vertical spacing between longitudinal bars and less a function of the overall depth. In addition, Collins and Kuchma showed that high-strength concrete members displayed a more significant size effect in shear than normal-strength concrete members.

To date, no published studies have been found on the size effect in shear for hollow-core units that contain no transverse or longitudinal mild-steel reinforcement and, depending on the manufacturer, employ high-strength concrete. A size-effect study was undertaken with data from five published experimental programs^{9,15-18} and recent test programs by two U.S. manufacturers. A total of 198 units were included, ranging in depth from 7.87 in. to 19.7 in. (200 mm to 500 mm). **Table 1** shows the relevant information pertaining to the hollow-core units used in this study.

Figure 2 shows a plot of the normalized shear stress at failure versus overall depth for all hollow-core units included in this study, encompassing all void types and prestressing levels. This plot does not suggest a size effect in shear given the wide spread of the data. However, to get a more accurate portrayal of a possible size effect, the comparison should be made between units of different

Table 1. Hollow-core-unit information for size-effect study

Unit depth h , in.	Number of specimens per void type			Concrete compressive strength f'_c , psi		Normal stress due to prestress f_{pc} , psi	
	Circular void	Noncircular void	Total	Minimum	Maximum	Minimum	Maximum
7.87–8.66	4	108	112	6000	8323	293	756
10–10.43	23	11	34	6000	7568	262	917
11.81–12.6	5	18	23	5126	7859	327	996
14.6–16	0	23	23	6000	10,830	332	928
19.7	0	6	6	7813	8172	624	837

Note: f_{pc} = compressive stress in concrete at centroid of cross section resisting externally applied loads after allowance for all prestress losses. in. = 25.4 mm; 1 psi = 6.895 kPa.

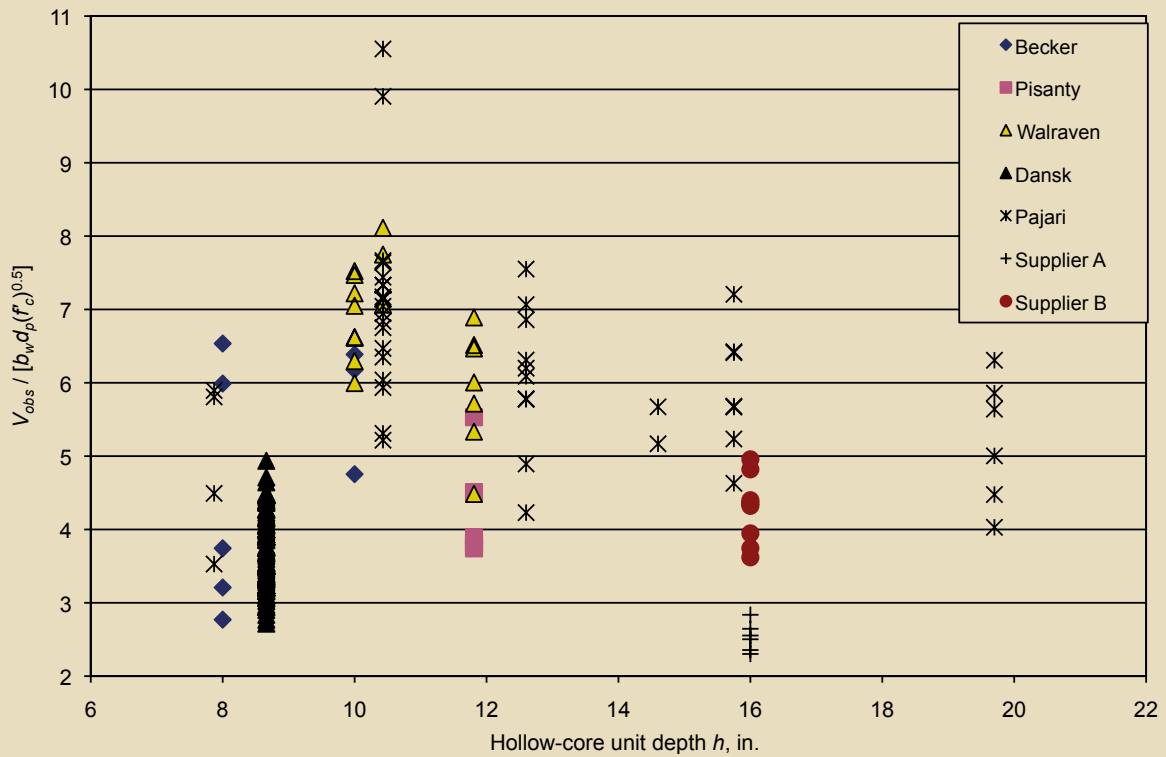


Figure 2. This graph plots the normalized shear stress at failure versus unit depth for all void types and prestress levels. Note: b_w = web width; d_p = distance from extreme compression fiber to centroid of prestressing steel; f_c = specified compressive strength of concrete; V_{obs} = experimentally observed failure shear at critical point. 1 in. = 25.4 mm.

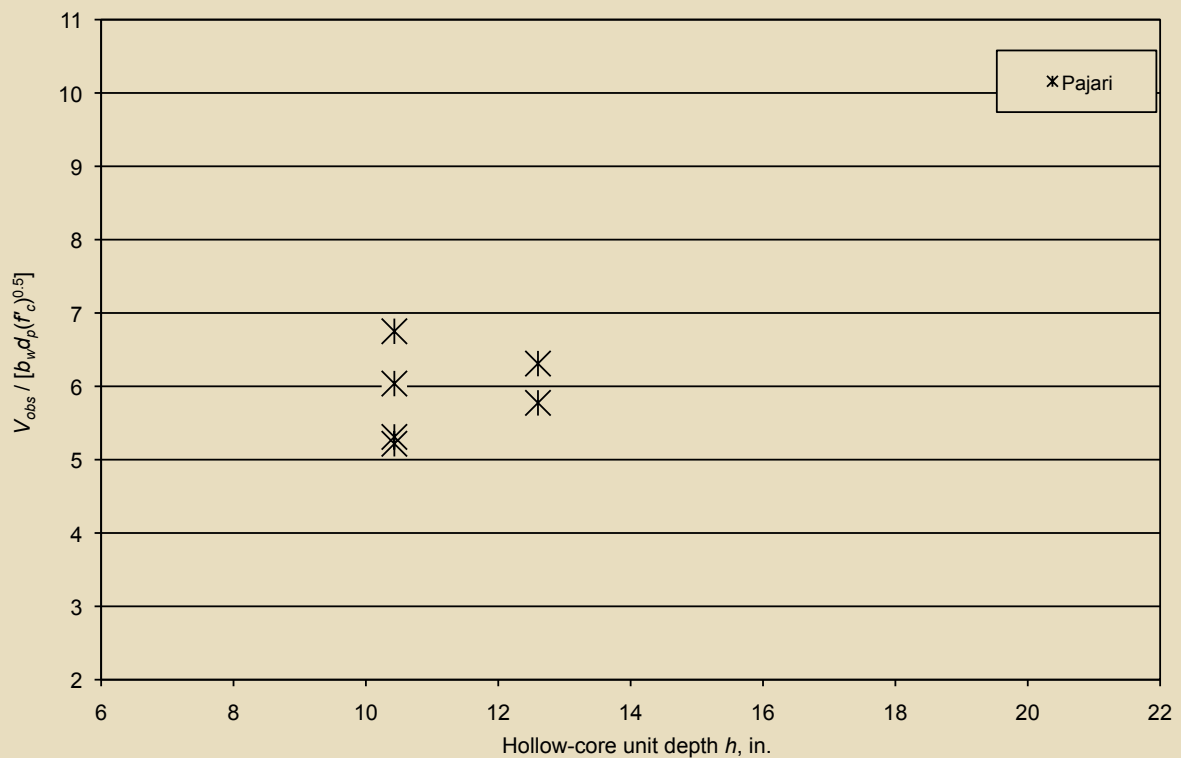


Figure 3. This graph plots the normalized shear stress versus slab depth for circular void types. Note: b_w = web width; d_p = distance from extreme compression fiber to centroid of prestressing steel; f_c = specified compressive strength of concrete; V_{obs} = experimentally observed failure shear at critical point. 1 in. = 25.4 mm.

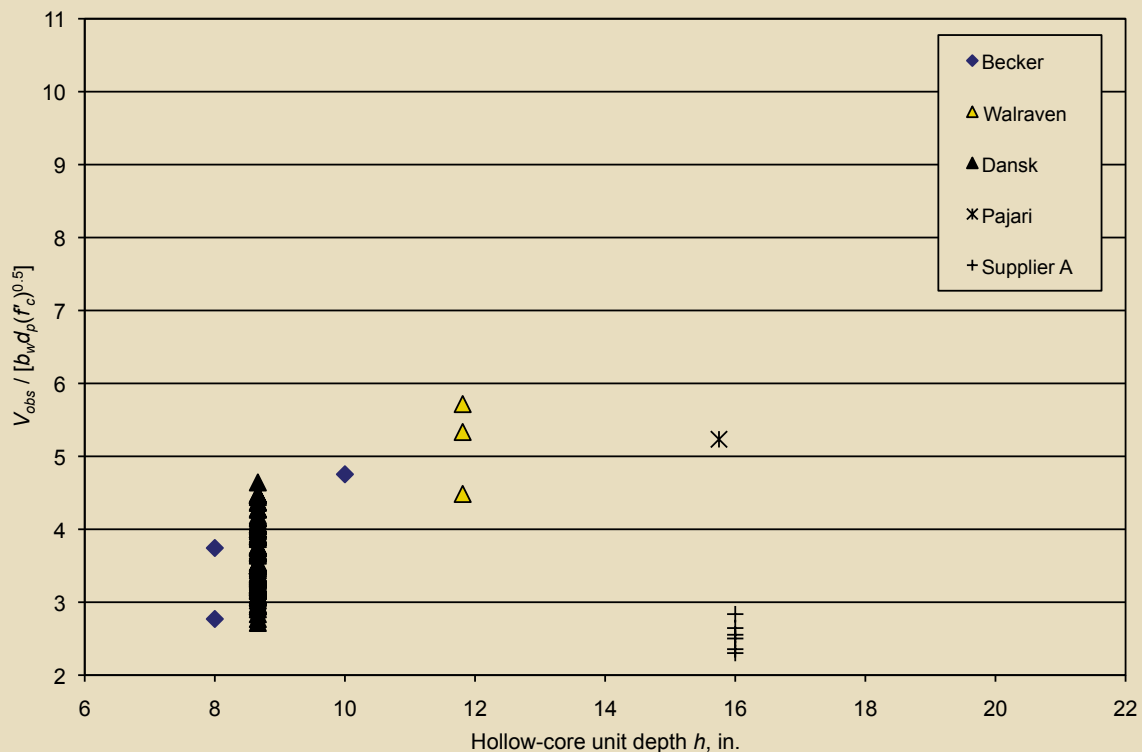


Figure 4. This graph plots the normalized shear stress versus slab depth for noncircular void types. Note: b_w = web width; d_p = distance from extreme compression fiber to centroid of prestressing steel; f_c' = specified compressive strength of concrete; V_{obs} = experimentally observed failure shear at critical point. 1 in. = 25.4 mm.

depths with similar void types and prestressing levels. To this end, the hollow-core units were categorized by void type—circular or noncircular—and by prestressing level. Three different levels of prestress were used as indicated by the value of f_{pc} . This value of stress arises from the fully developed force in the strand at the end of the transfer length, assuming 15% prestress loss divided by the gross cross-sectional area of the unit.

Figures 3 through **7** show plots of the normalized shear stress versus member depth for hollow-core units categorized in the manner described previously. These figures do not indicate a size effect in shear for hollow-core units up to 20 in. (510 mm) in overall depth due, once again, to the spread of the data. There does not appear to be a trend in the majority of the cases that is discernible beyond the magnitude of scatter in the test data. In some cases, such as Pajari's⁹ tests in Fig. 5, there appeared to be a trend in which normalized shear strength actually increased with increasing hollow-core-unit depth. However, Walraven's¹⁵ tests in Fig. 7 suggested a size effect. The scatter in the normalized shear stress was considerable between units of the same depth, and the ratio of the maximum normalized shear stress to the minimum was on the order of two for many of the hollow-core-unit depths for each testing program. This magnitude of scatter is consistent with that observed in a size-effect study of nonprestressed beams that was conducted by Bentz.¹⁹ Besides the usual vari-

ability of material properties for concrete, the scatter can be attributed to differences in fabrication and the ways in which the tests were conducted, analyzed, and reported by the various sources.

Geometry of cross section

Hollow-core units are produced with a variety of void shapes, but voids can be generally categorized into two types: circular and noncircular. The exact shapes of the noncircular voids vary among manufacturers. **Figure 8** shows two different noncircular void types from different manufacturers. The effect of the void type on the web-shear capacity of hollow-core units has been noted by a number of researchers and has been studied by Yang¹⁰ and Pajari.⁹ Three different aspects of cross-section geometry on web-shear strength are discussed in the next sections.

Location of critical point Traditional web-shear-design procedures, such as the one suggested by ACI 318-08 and ACI 318-05 and Eurocode 2, make a number of simplifying assumptions. The first assumption is that the location of the maximum principal tensile stress—the critical point—occurs at the centroid of the section at a location of $h/2$ from the face of the support. At this point, the beneficial effects of the vertical normal stresses due to the reaction are assumed to be negligible. The shear stress is a maximum based on the mechanics of linearly elastic mate-

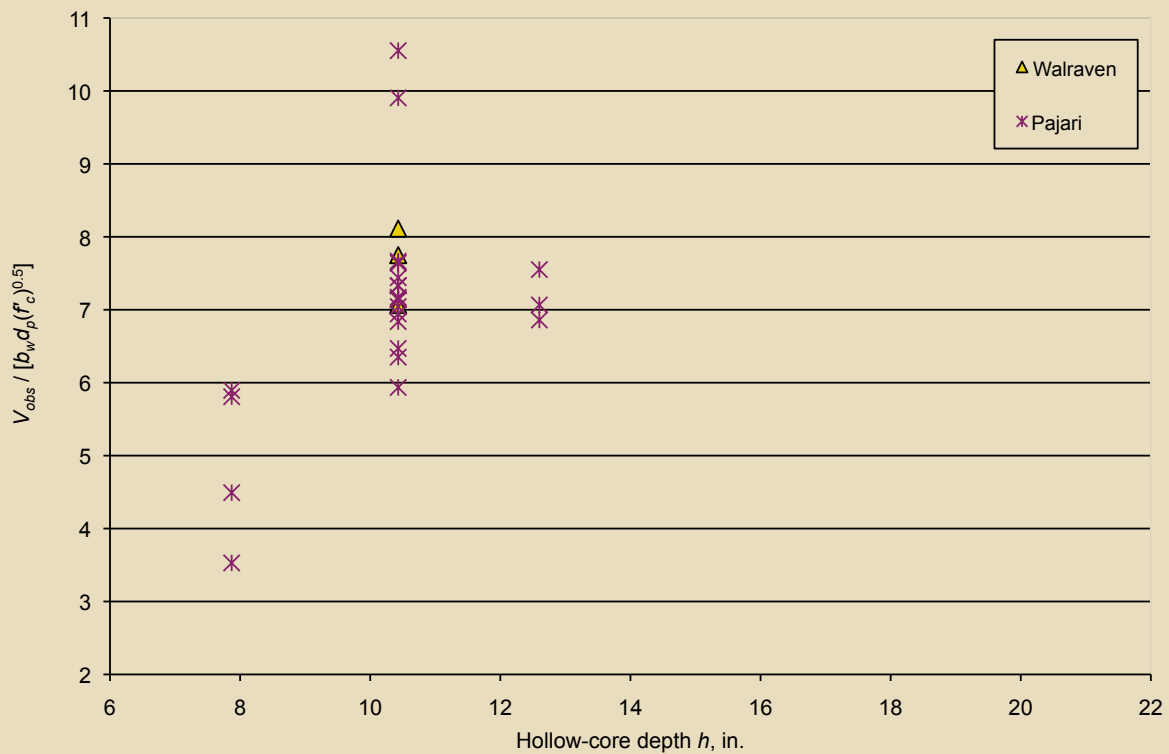


Figure 5. This graph plots the normalized shear stress versus slab depth for circular void types. Note: b_w = web width; d_p = distance from extreme compression fiber to centroid of prestressing steel; f'_c = specified compressive strength of concrete; V_{obs} = experimentally observed failure shear at critical point. 1 in. = 25.4 mm.

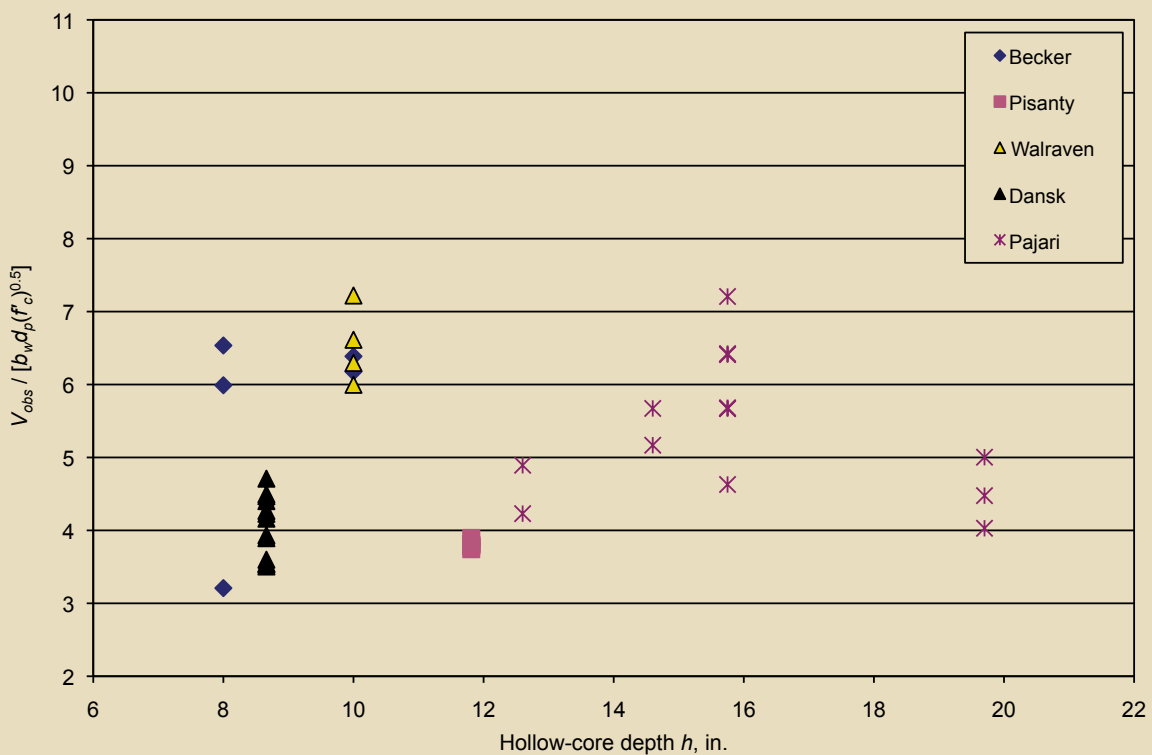


Figure 6. This graph plots the normalized shear stress versus slab depth for noncircular void types. Note: b_w = web width; d_p = distance from extreme compression fiber to centroid of prestressing steel; f'_c = specified compressive strength of concrete; V_{obs} = experimentally observed failure shear at critical point. 1 in. = 25.4 mm.

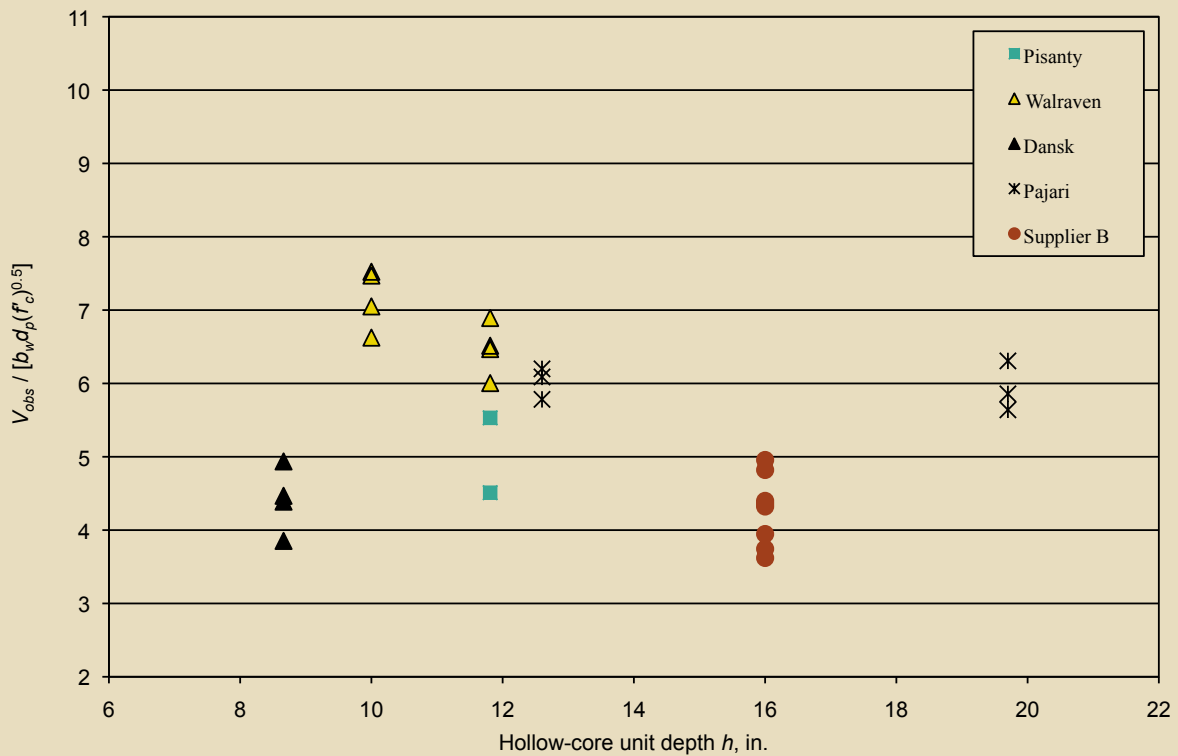
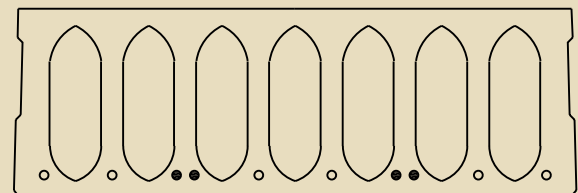


Figure 7. This graph plots the normalized shear stress versus slab depth for noncircular void types. Note: b_w = web width; d_p = distance from extreme compression fiber to centroid of prestressing steel; f_c = specified compressive strength of concrete; V_{obs} = experimentally observed failure shear at critical point. 1 in. = 25.4 mm.

rials, and the flexural stresses in the section due to external loads and prestress are minimized.

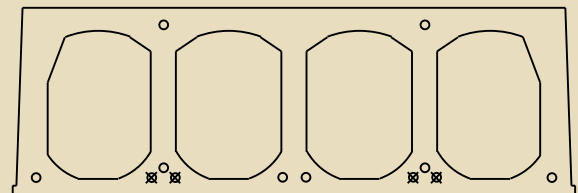
Yang¹⁰ showed that the previous assumptions may not be valid for hollow-core units. Yang performed linear two-dimensional and three-dimensional finite-element analyses of 22 I-shaped members that mimicked strips of hollow-core units. Four different cross sections were analyzed, two with circular voids and two with noncircular voids. The units had depths of 7.9 in., 10.4 in., and 15.8 in. (200 mm, 265 mm, and 400 mm) with varying levels of prestressing force and a parabolic prestressing force transfer curve. Yang determined that the horizontal location of the critical section for circular voids occurred at the intersection of the centroid and a line drawn at 35 deg from the horizontal of the center of the support. For sections with noncircular voids, the critical point occurred at the intersection of the same 35-deg line with the web and bottom flange. This finding results in at least four important implications for hollow-core units with noncircular voids:

- The prestressing force at this critical point is smaller than that used by ACI 318-08 and ACI 318-05 because the critical point is closer to the end of the member in the transfer zone.
- Under uniform loading, the shear force is larger at locations close to the support. The effect is unimportant.



- 0.5-in.-diameter strand
- 0.5-in.-diameter debonded strand

Supplier A hollow-core unit



- ⊗ 0.6-in.-diameter strand
- 0.5-in.-diameter strand

Supplier B hollow-core unit

Figure 8. The exact shapes of the noncircular voids vary among manufacturers, including these two different noncircular void types, each produced by a separate manufacturer. Note: 1 in. = 25.4 mm.

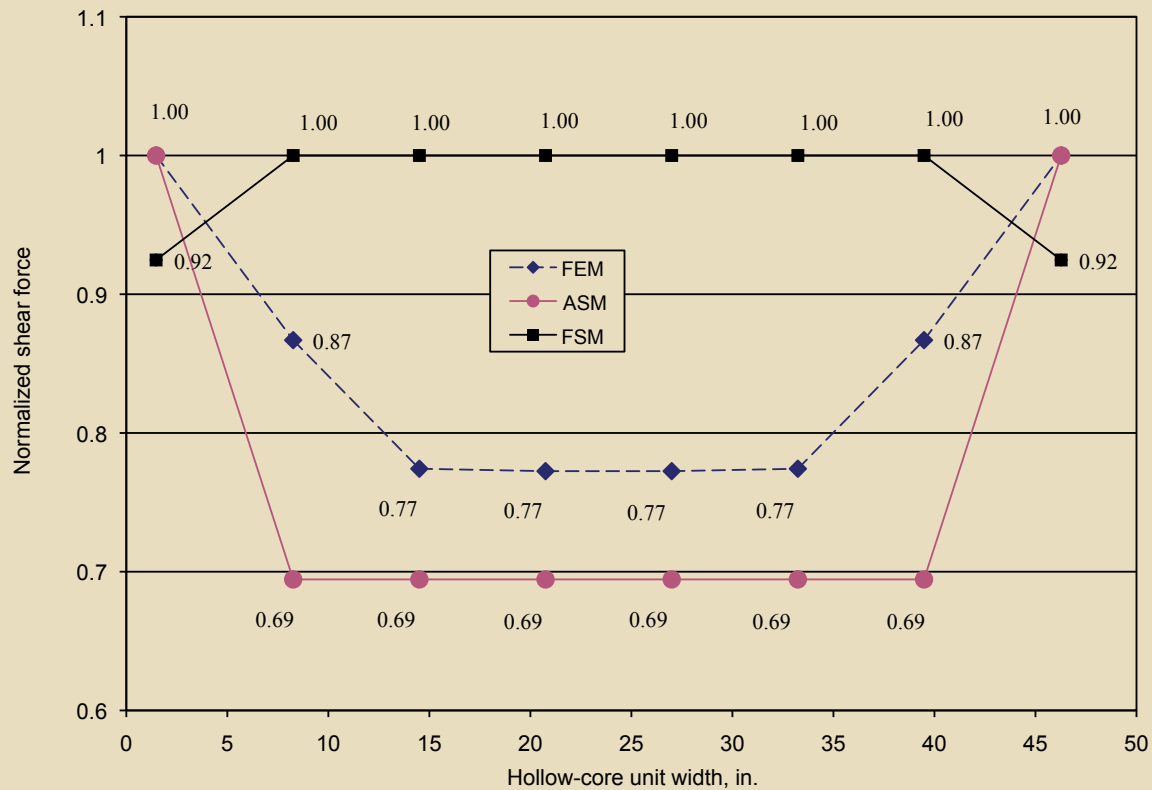


Figure 9. This graph shows the normalized web-shear distribution for supplier A hollow-core units. Note: ASM = axial stiffness method; FEM = finite-element model; FSM = flexural stiffness method. 1 in. = 25.4 mm.

ant for a member with large point loads relative to uniform loading because the shear force will be essentially constant.

- Tensile flexural stresses will exist at the critical point due to the external loads.
- Compressive flexural stresses exist at the critical point due to eccentricity of prestressing.

The first three points tend to decrease the calculated web-shear capacity, while the fourth tends to increase it. The relative difference between these will ultimately determine the net effect on the shear capacity. Calculations by the author, Yang, and Pajari show that the shear capacities will always be smaller than those obtained using ACI 318-05 or a similar Eurocode 2 equation, and the reduction of the prestressing force represents a reduction of the web-shear strength of as much as 15%. For example, the prestressing force at Yang's critical point was up to 40% smaller than that at ACI 318-05's critical point for supplier B's units, assuming a bearing length of 4 in. (102 mm), no overhang, and a linear change in prestressing force over the transfer length.

Transverse distribution effect Traditional methods for predicting the web-shear capacity of hollow-core units use the sum of the individual web widths in the capacity

expressions. This implies an even distribution of shear to the individual webs and uniform precompression in each web. However, variability in the widths of the individual webs, either by design or due to the manufacturing process, may result in an uneven distribution of shear to the webs. Jonsson²⁰ recognized this effect in his formulation by using the capacity of the highest-stressed web multiplied by the ratio of the total hollow-core-unit width divided by the tributary flange width of the weakest web. Jonsson assumed that the distribution of the shear to the webs is based on the flexural rigidity of the individual webs and their tributary flanges. Under this assumption, the most highly stressed webs are the interior webs with the largest flanges. This is the flexural stiffness method. It resulted in the interior webs being equally stressed, and the exterior webs were stressed to 50% of the stress in the interior webs for the units that he analyzed. Another simplified method of calculating the web-shear distribution would be to base stress on the vertical axial stiffness of the individual webs at the bearing location. In this manner, the thicker webs would resist more load than the thinner webs. This method is the axial stiffness method.

Linear, three-dimensional, finite-element analyses of typical hollow-core units performed by the authors in the current study do not agree with either of these methods. Two hollow-core units, one from supplier A and one from supplier B (Fig. 8), were analyzed using the finite-element-

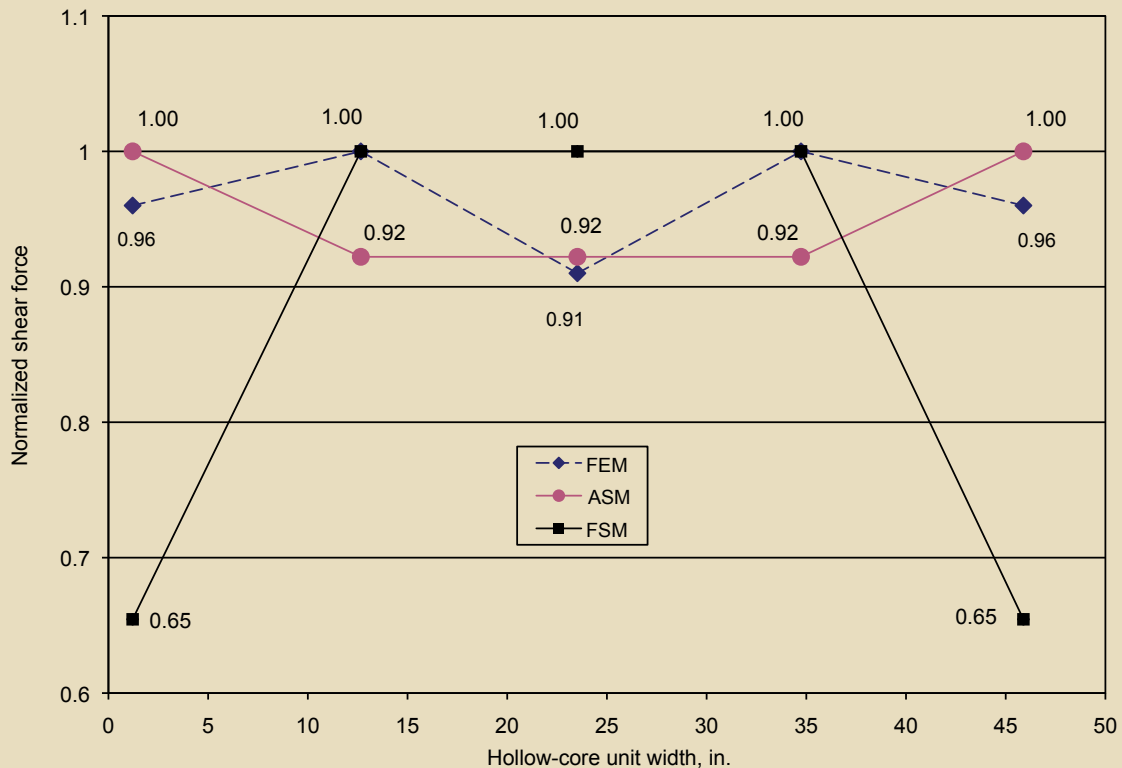


Figure 10. This graph shows the normalized web-shear distribution for supplier B hollow-core units. Note: ASM = axial stiffness method; FEM = finite-element model; FSM = flexural stiffness method. 1 in. = 25.4 mm.

analysis program ABAQUS. A linear-elastic, three-dimensional analysis was performed using eight-node brick elements, about 1/2 in. wide (13 mm) on each side at and near the support, with reduced integration. The prestressing strands were not modeled because it was thought that the effect of the strands would be minimal in the vertical direction and not worth the additional computational cost. The web-shear distribution was calculated in two ways. The first procedure involved integrating the vertical normal stress across each web occurring at the web-flange intersection directly above the inside face of the support. The second procedure involved integrating the bearing stresses at the support tributary to each web (center to center of the voids). The largest difference between the two procedures was less than 5%.

Figures 9 and 10 compare the normalized web-shear distribution based on the first procedure of the finite-element analysis with the results from the flexural and axial stiffness methods. The distribution of web shear from the finite-element analysis for the units from supplier A was not uniform. The four interior webs absorbed 23% less shear than the exterior webs. The distribution for the units from supplier B was nearly uniform, with the central web resisting 9% less shear than the first interior webs.

Given the uneven shear distribution for the units from supplier A coupled with the shear lag of the prestressing force

across the width and the possibility of debonded strands, it is conceivable that a highly stressed web, with little or no precompression, will fail prior to the other webs. Shear redistribution will then occur, and if the remaining webs cannot resist this extra load, an unzipping failure will occur at a load less than that predicted by traditional methods. A prediction of the shear capacity of the hollow-core units from both suppliers was made based on the web-shear stress distribution from the finite-element analysis and the capacities of the individual webs based on the prestressing force available only in each respective web. The results of this will be discussed in more detail in the section “Disparity Between Manufacturers.”

Effect of cross-section geometry on shear stress The parameters I , Q , and b_w , which are typically unique for each supplier, and d_p affect the shear capacity. These parameters are best explained with reference to the expression for the shear stress in a section derived from a mechanics-of-materials approach. This shear stress can be expressed as Eq. (1).

$$v = \frac{VQ}{b_w I} \quad (1)$$

The first area moment Q is a function of the distance from the centroid, and it reaches a maximum value at the centroid. This shear distribution is parabolic, with the

maximum shear stress occurring at the centroid. Eurocode 2 uses this expression for the shear stress in its web-shear expression.

The ACI 318-08 and ACI 318-05 provisions use the average or nominal shear stress in the section, which is expressed as Eq. (2).

$$v = \frac{V}{b_w d_p} \quad (2)$$

This results in a constant, average value of the shear stress throughout the depth.

For a given value of concrete tensile strength, the use of the average shear stress described by Eq. (2) will result in a higher predicted shear strength relative to that predicted using the shear stress in Eq. (1). The reason for this difference is that the ratio V/Q is smaller than d_p . The ratio V/Q is $0.77d_p$ for a rectangular section, assuming d_p is $0.9h$, and it ranged from $0.8d_p$ to $0.9d_p$ for the hollow-core units analyzed by Pajari⁹ and the author. The value for this ratio for the units from supplier A was $0.8d_p$, while the ratio for the units from supplier B was $0.88d_p$.

Axial stress due to prestress

Axial compressive force in a concrete section tends to increase its web-shear capacity, and this phenomenon can easily be understood from stress analysis using Mohr's circle of a point in the member under combined shear and a uniaxial compressive stress. A complete description of this analysis may be found in textbooks on reinforced concrete design (for example, Nilson²¹). The compressive stress tends to reduce the principal tensile stress, causing an increase in capacity because a web-shear failure occurs when the principal tensile stress reaches the limiting tensile strength of the concrete. The problem then becomes the determination of the correct prestressing force to use for resisting a specific design shear force.

At the ends of prestressed members, there is no force in the prestressing strands due to lack of end bearing and the large bond stresses that are required to transfer the force from the steel to the concrete. As a result, the force in the strand is gradually transferred to the concrete, resulting in a prestressing-force gradient that increases with distance from the ends. The total distance required for the complete transfer of prestressing force is called the transfer length L_t . The location of the maximum principal tensile stress (that is, critical point) in hollow-core units, which has traditionally been taken at a horizontal distance $h/2$ from the face of the support, is typically within the transfer length of the strands used in current practice. Therefore, the magnitude of the prestressing force in the critical section is bounded by zero and the fully effective value at the end of the transfer length.

Numerous researchers²²⁻³³ have attempted to determine the transfer length of prestressing strands, the shape of the prestressing-force gradient, and the parameters that affect these quantities. There is general agreement among researchers on the parameters that affect the transfer length, and these include the size and spacing of the strands, concrete strength, method of release, initial prestressing force, and the surface condition of the strand. However, section 11.4.4 of ACI 318-08 and ACI 318-05 explicitly considers only the diameter of the strand, with the expression for the transfer length of the strand being approximated as $50d_b$, where d_b is the nominal diameter of the prestressing strand. Existing test results sometimes show large variations between the measured transfer lengths and those calculated per section 11.4.4 of ACI 318-08 and ACI 318-05.

The observed shape of the prestressing-force gradient is another parameter that varies among research studies. Some exhibited a parabolic transfer curve, and others exhibited a linear relation.²⁹ It is unclear if any of this research, which dealt almost exclusively with precast, prestressed concrete girders and small rectangular sections, can be applied to extruded hollow-core units because these generally use a dry, no-slump concrete with different properties and compaction than those tested in the transfer-length research. Only one published test¹⁵ on the transfer length of prestressing strands in hollow-core units was found. The transfer lengths were determined by measuring the concrete surface strains after sawing through a hollow-core unit to release the prestressing force. The measured transfer lengths were $32d_b$ on one side of the cut and $40d_b$ on the other side of the cut, and the shape of the transfer curves was closer to linear than parabolic. The age of the unit at the time of testing, which affects the transfer length, was not published.

From a design standpoint, it is conservative to use a longer transfer length and a linear prestressing-force curve because these assumptions result in a lower prestressing force in the section. However, from a research point of view, it is desirable to have an accurate model for this mechanism in order to quantify the effects of the other parameters that affect the shear capacity. Lacking sufficient data on the transfer length of hollow-core units, the analyses conducted in this paper were done assuming a linear prestressing force transfer curve (that is, constant bond stress) consistent with ACI 318-08 and ACI 318-05 recommendations.

Tensile strength of web concrete

The general theory for unreinforced concrete members failing in web shear assumes that the members fail when the maximum principal tensile stress reaches the limiting tensile strength of the concrete. Thus, the concrete tensile strength is arguably one of the most important parameters for assessing the web-shear capacity. However, Tasuji et

al.³⁴ also argued that the most appropriate failure criterion is a limiting tensile strain. A limiting tensile stress was assumed in this study, given the history of its use in design codes. The problem is to determine the correct value of this limiting tensile stress and how to measure it with standard material tests.

The stress state in the webs of hollow-core units consists of biaxial principal tension and compression. It has been shown³⁴⁻³⁶ that the tensile strength of concrete is reduced in the presence of a compressive stress acting orthogonally to the tensile stress. Thus, the limiting tensile stress under this biaxial stress state produced by shear is different from that under a uniaxial case.

Evaluation of a large number of beam tests³⁷ showed that diagonal tension cracks formed at an average shear stress equal to about $3.5\sqrt{f'_c}$, where f'_c is the specified compressive strength of concrete. Thus, ACI 318-08 and ACI 318-05 specify a value of $3.5\sqrt{f'_c}$ in the expression for web-shear cracking for prestressed members. The relationship between the tensile strength of concrete and its uniaxial compressive strength has been shown to be dependent on the concrete, the compaction technique, and the curing method.³⁸ These factors make it difficult to obtain the correct tensile-strength value to be used in the formulation of a web-shear-capacity expression given the fact that these factors can vary considerably among manufacturers.

Given the nature of the dry mixture and casting method used in hollow-core-unit production, it is also possible that there is a nonuniform level of compaction throughout the depth of the unit for some manufacturers. This could result in varying levels of concrete strength throughout the depth that may affect the shear capacity and the transfer length.

Pisanty and Regan³⁹ demonstrated the variability of concrete strength throughout the depth in 7.9-in.-deep and 11.8-in.-deep (200 mm and 300 mm) hollow-core units. They performed modulus-of-rupture tests on webs sawed from hollow-core units. The prestressing tendons were only left out of the webs that were sawed and tested. They also tested units in which the prestressing strands were left out of all of the webs. The authors implied that the units were the extruded type, but it was not explicitly stated. The webs were sawed from the units and then sawed again at the midheight of the web. These were then loaded at the $1/3$ points in various configurations. The configurations consisted of placing the top of the web, the middle of the web, and the bottom of the web in tension to determine the variability of tensile strength.

Pisanty and Regan³⁹ found that the modulus of rupture at the center of the 7.9-in.-thick (200 mm) units was 16.8% less than at the top of the unit for the unit with prestressing, and 11.7% less for the 7.9-in.-thick units without prestressing. The 11.8-in.-thick (300 mm) units exhibited similar

behavior but with a smaller difference in tensile strength: the difference in tensile strength between the center and top of the unit was 10.8% for the prestressed unit and 4.7% for the unit without prestressing. The greater tensile strength again occurred at the top of the unit. It is unclear whether this trend exists for deeper hollow-core units because no tests on sections thicker than 11.8 in. were found in the literature. It is also possible that this difference varies among manufacturers, as their mixture proportions and manufacturing processes (including curing) are not all the same.

Shear lag of prestressing force

Near the support, the compressive stresses in the section at points directly above the strands are less than the stress at the level of the strands due to the deformation of the section. This effect is known as shear lag and theoretically does not occur in a perfectly rigid section. If the prestressing force is assumed to spread into the section at 45 deg, the normal stress in the section's centroid at the ACI 318-08 and ACI 318-05 critical point could be reduced by as much as 50% from the stress that would result without shear lag.

The effect is less dramatic if the critical point is at the location found by Yang. In this case, the stress in the section at the critical point would be reduced about 25%, depending on the section geometry. To date, no studies have been found that quantify this effect in hollow-core units. ACI 318-08 and ACI 318-05 and other design guidelines do not account for shear lag in their shear-capacity expressions. The effect would obviously reduce the estimated shear capacity because the precompression in the section is reduced. Walraven and Mercx¹⁵ accounted for shear lag in their formulation by assuming that the stress due to prestress at the critical point occurred at the inside face of support, which implied a force spread of 45 deg into the section because their critical point was at $h/2$ from the inside face of support. This vertical-shear-lag effect was ignored in the current study.

Shear lag not only occurs throughout the depth of the unit but also across the width. It is not uncommon to have different amounts of prestressing below individual webs in a hollow-core unit. In addition, some manufacturers debond a number of strands for a distance beyond the critical point in order to limit the stresses at transfer at the end of the unit to prevent end splitting. As a result, some webs in the unit may not have any precompression, or a smaller value of precompression may be present at the critical point because there is insufficient distance for the force from the adjacent stressed strands to reach the unstressed or less-stressed webs. Therefore, there is not a uniform precompression across the width of the unit, which is an important assumption in the ACI 318-08 and ACI 318-05 shear provisions. As a result, the shear capacities of the

individual webs in a unit may differ. This horizontal-shear-lag effect was considered for this study and is described in a following section.

Shear span-to-depth ratio a/d

The shear capacity of concrete members is affected by the shear span-to-depth ratio a/d_p of the member.⁴⁰ This effect is attributed to the arching action that takes place when the load is applied close to the support. This behavior has little effect on the web-shear capacity of prestressed members with a/d_p greater than 2.4⁴¹ and therefore was neglected in the present analysis because all of the shear tests considered had a/d_p no smaller than 2.4.

Plant tests versus shear-prediction methods

In 2003 and 2004, two U.S. manufacturers performed shear tests on their own 16-in.-thick (410 mm) hollow-core units. Supplier A tested both ends of three units to failure for a total of six tests. All of the units failed in web shear. The mean value of the ratios of observed failure shear forces V_{obs} to calculate shear capacities per ACI 318-05 V_{pre} was 0.61 with a coefficient of variation (COV) of 0.08. This ratio based on ACI 318-08 was 1.22 with the same COV of 0.08.

Supplier B tested 10 units to failure. Eight of the units failed in web shear, and two failed in flexure shear. The two units that failed in flexure shear did so at a load about 25% greater than that predicted by the ACI 318-05 flexure-shear expression. Six of the eight units that failed in web shear did so at loads less than those predicted by the ACI 318-05 web-shear expression. For the units from supplier B, the mean value of the ratios of V_{obs}/V_{pre} per ACI 318-05 was 0.91 with a COV of 0.12. This ratio based on ACI 318-08 was 1.82 with the same COV of 0.12.

Figure 8 shows the hollow-core unit geometry along with the strand configuration from supplier A. Four of ten strands were debonded over a length of 2 ft (0.6 m) from the end and were stressed to 65% of their tensile strength. Figure 8 shows a hollow-core-unit section, for which none of the strands were debonded, from supplier B. The bottom strands were stressed to 70% of tensile strength, while the top two strands were stressed to 30% of tensile strength.

Table 2 shows the relevant parameters for all units tested. Supplier B performed two cylinder tests from the concrete batch used for each unit and also measured the web widths for each unit. Supplier A provided the specified compressive strength and the nominal web widths. All strands used by the suppliers had an ultimate tensile strength of 270 ksi (1860 MPa).

The observed shear capacities from the above tests were compared with the shear capacities predicted by five different methods: ACI 318-05, Eurocode 2, modified compression field theory, AASHTO LRFD specifications, and Yang's method. Web shear was the only failure mode considered in this comparison. Comments on the ACI 318-08 will also be made at the end of the section.

ACI 318-05

ACI 318-05 Eq. (11-12) provides an expression for the nominal web-shear cracking strength V_{cw} of prestressed concrete members.

$$V_{cw} = \left(3.5\sqrt{f'_c} + 0.3f_{pc} \right) b_w d_p + V_p$$

ACI 318-05 Eq. (11-12)

where

V_p = vertical component of effective prestressing force at critical section

For hollow-core units, V_p equals zero because draped or harped strands are not used. ACI 318-05 Eq. (11-12) assumes a constant average shear stress throughout depth d_p and width b_w of the webs, and the term in parentheses is an approximation of the quadratic expression that results from Mohr's circle analysis for the principal tensile stress.²¹

Eurocode 2

Equation (6.4) from section 6.2.2 in Eurocode 2 provides the following expression for the web-shear cracking strength of prestressed concrete members $V_{Rd,c}$:

$$V_{Rd,c} = \frac{Ib_w}{Q} \sqrt{\left(f_{ctd} \right)^2 + \alpha_l \sigma_{cp} f_{ctd}}$$

Eurocode 2 Eq. (6.4)

where

f_{ctd} = design tensile strength of concrete

α_l = ratio of distance from end of member to transfer length

σ_{cp} = fully effective concrete compressive stress at the centroid due to prestressing

Eurocode 2 Eq. (6.4) is fundamentally similar to ACI 318-05 Eq. (11-12), but for the shear-stress distribution it uses the exact quadratic expression derived from mechanics-of-materials (that is, Mohr's circle) stress analysis, represented by the I/Q term, instead of the constant average shear stress from the linear approximation adopted by ACI 318-05 Eq. (11-12). Note that f_{ctd} is the tensile strength of

Table 2. Hollow-core unit information for U.S. manufacturers

Supplier	Test no.	f'_c , psi	b_w , in.	V_{obs} at $h/2$, kip	Span L , ft	Shear span a , in.	Effective depth d_p , in.	a/d_p
A	1a	6000	15.9	49	25.67	36	15	2.4
	1b	6000	15.9	43.64	25.67	60	15	4
	2a	6000	15.9	47.3	25.67	60	15	4
	2b	6000	15.9	46.35	25.67	36	15	2.4
	3a	6000	15.9	42.64	25.67	36	15	2.4
	3b	6000	15.9	52.54	25.67	60	15	4
B	1	10,830	11.81	61.7	15	44.5	13.9	3.2
	2	9310	11.69	68.8	15	44.5	13.9	3.2
	3	8760	11.69	56.8	15	80.5	13.9	5.8
	4	8930	11.5	65.7	15	44.5	13.9	3.2
	5	10,300	11.72	79.5	27	80.5	13.9	5.8
	6	10,765	11.78	84	27	80.5	13.9	5.8
	7	9730	11.88	70.2	15	59	13.9	4.3
	8	9985	11.74	46	15	59	13.9	4.3

Note: b_w = web width; f'_c = specified compressive strength of concrete; h = overall thickness or height of member; V_{obs} = experimentally observed failure shear at critical point. 1 in. = 25.4 mm; 1 ft = 0.305 m; 1 kip = 4.448 kN; 1 psi = 6.895 kPa.

concrete reduced by a material factor. However, for the purposes of this comparison, the tensile strength was not reduced by this factor because none of the other methods considered the applicable code strength reductions.

Modified compression field theory

Vecchio and Collins^{12,13} developed the modified compression field theory to predict the behavior of concrete elements under a state of two-dimensional stress. The theory can be applied to prestressed concrete flexural members under the actions of shear, moment, and axial load. The modified compression field theory treats cracked concrete as a different material than uncracked concrete, with its own constitutive relationships. Equilibrium, compatibility, and constitutive relationships are formulated in terms of average stresses and average strains taken over a distance on the element that includes several cracks.

The solution method is somewhat cumbersome and is not well suited for hand calculations because 15 equations need to be solved. However, Collins and Bentz^{42,43} developed a computer program that implements the modified compression field theory. This program was used to predict the shear capacities of the unit tests analyzed in the following section. The program cannot analyze hollow-core units in their entirety, so the units were divided into discrete I-sections, and the total hollow-core unit capacity is the sum of the capacities of each section.

AASHTO LRFD specifications

In 1998, AASHTO adopted a new shear-design method for incorporation into the AASHTO LRFD specifications. The method is a simplified form of the modified compression field theory. It is in a form that is familiar to engineers who have experience using ACI 318-05 and the previous AASHTO LRFD specifications.

$$V_n = V_c + V_s + V_p$$

where

V_n = nominal shear strength

V_c = nominal shear resistance of concrete

V_s = nominal shear resistance of transverse reinforcement

The V_s and V_p terms are zero for hollow-core units, which have no shear reinforcement and use straight tendons. The web-shear strength expression then reduces to Eq. (3).

$$V_n = 0.0316\beta\sqrt{f'_c}b_wd_p \quad (3)$$

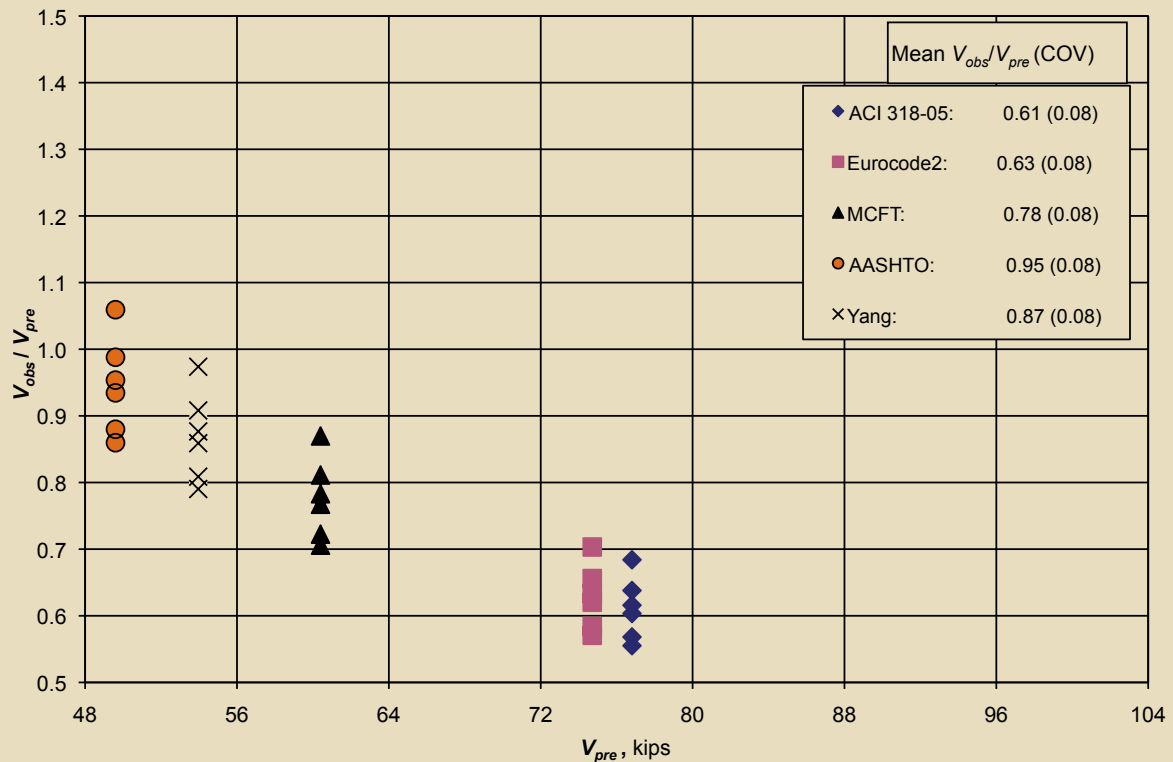


Figure 11. This graph compares all of the methods of predicting shear capacities for supplier A's hollow-core units. Note: MCFT = modified compression field theory; V_{obs}/V_{pre} = ratio of observed to predicted shear strengths; V_{pre} = predicted shear strength. 1 kip = 4.448 kN.

where

β = factor indicating ability of diagonally cracked concrete to transmit tension

The coefficient β is a function of the longitudinal strain in the member, which is dependent on the orientation of the principal stresses. The values of β tabulated in the AASHTO LRFD specifications were determined by calculating the stresses that can be transmitted across diagonally cracked concrete. As the cracks widen, the amount of stress that can be transmitted across them decreases. Thus, an increase in the longitudinal strain results in a decrease in β and, therefore, a decrease in the shear capacity. While this is a simplified version of the modified compression field theory, it still requires iteration to obtain the shear capacity.

Yang's method

Yang¹⁰ presented a procedure to predict the web-shear capacity of hollow-core units. As in ACI 318-05 and Eurocode 2, a web-shear failure was assumed to occur when the principal tensile stress at the critical point reaches the limiting tensile strength of the concrete. Unlike ACI 318-08, ACI 318-05, and Eurocode 2, the shear stresses induced by the prestressing-force gradient were accounted for, and the location of the critical point was not taken at the centroid

but at the location previously described in the section discussing the effect of the geometry of the section and the location of the critical point. This complicates the analysis because there are more terms in the horizontal equilibrium equations used to derive the shear stress, and the normal stresses due to flexure do not equate to zero. Equation (4) was derived by Yang.

$$V_{yang} = \frac{b_w I}{S_{cp}} \left\{ \frac{b_w}{2S_{cp}} f_{ct} x_{cp} z_{cp} + \frac{S_{cp}}{b_w} \left(\frac{e}{I} - \frac{A_{cp}}{A_g S_{cp}} \right) \frac{\partial N_p}{\partial x} + \left[\left(\frac{b_w}{2S_{cp}} f_{ct} x_{cp} z_{cp} \right)^2 + \frac{\partial N_p}{\partial x} \left(\frac{e}{I} - \frac{A_{cp}}{A_g S_{cp}} \right) f_{ct} x_{cp} z_{cp} + \left(\frac{1}{A_g} - \frac{e z_{cp}}{I} \right) N_p f_{ct} + f_{ct}^2 \right]^{1/2} \right\} \quad (4)$$

where

A_{cp} = area of section above the critical point

e = eccentricity of strand measured from the centroid

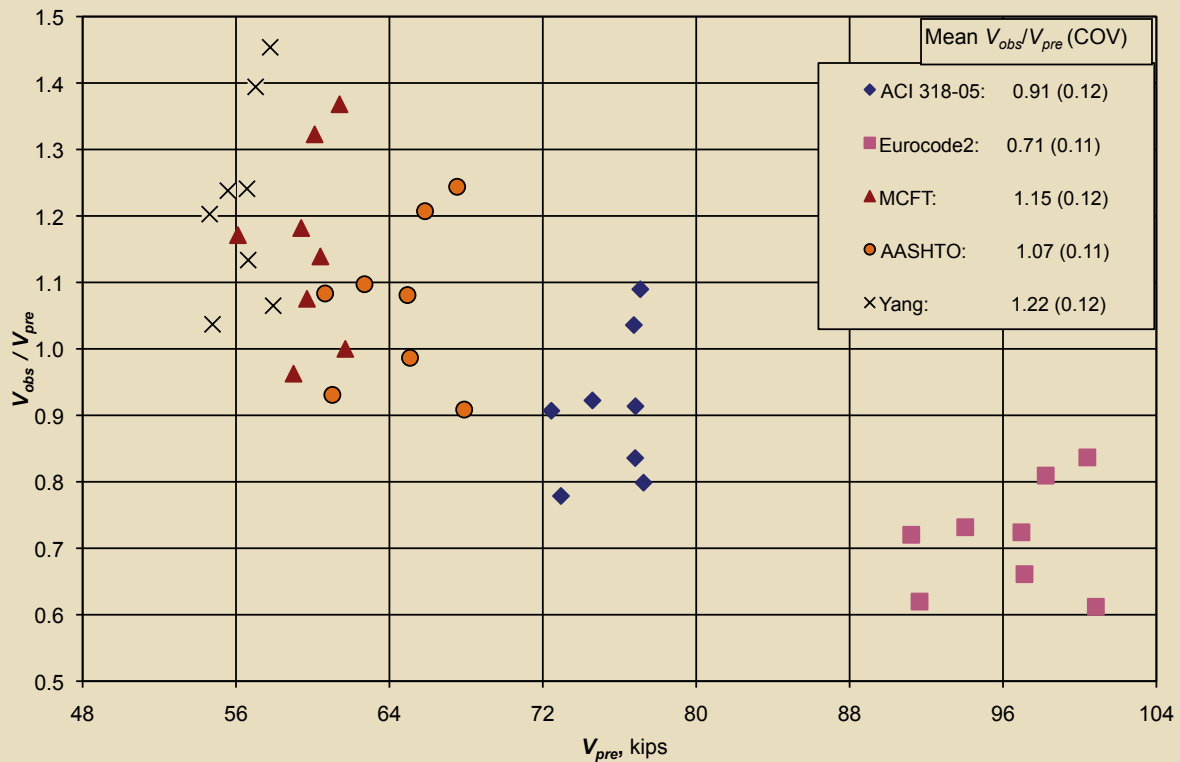


Figure 12. This graph compares all of the methods of predicting shear capacities for supplier B hollow-core units. Note: AASHTO = American Association of State and Highway Transportation Officials; COV = coefficient of variation; MCFT = modified compression field theory; V_{obs}/V_{pre} = ratio of observed-to-predicted shear strengths; V_{pre} = predicted shear strength. 1 kip = 4.448 kN.

N_p = prestressing force in strand

S_{cp} = first area moment of section about critical-point axis

V_{yang} = predicted web-shear strength for Yang's equation

x_{cp} = distance from center of support to critical point

z_{cp} = vertical distance from centroid to critical point

$\partial N_p / \partial x$ = prestressing-force gradient

Equation (4) reduces to the Eurocode 2 formulation if the critical point is at the centroid of the section and the shear stresses induced by the prestressing-force gradient are ignored.

Comparison of methods

The results from the comparison are shown graphically in **Fig. 11** and **12**. These figures show the ratio of observed shear strength V_{obs} to the predicted shear strength V_{pre} (V_{obs}/V_{pre}) plotted against the predicted shear strength V_{pre} . A ratio above unity indicates a safe prediction, while a ratio below unity indicates an unsafe one.

Figures 11 and 12 show that ACI 318-05 Eq. (11-12) provides the most unconservative prediction of web-shear

strength of all of the methods for the units from supplier A, followed by the Eurocode 2 estimates. For the units from supplier B, Eurocode 2 provides the most unconservative predictions of web-shear strength, followed by ACI 318-05 Eq. (11-12). There was a large disparity between the V_{obs}/V_{pre} between supplier A and supplier B for the majority of the methods. AASHTO LRFD specifications provided the best prediction for units from supplier A, while Yang's method provided the most conservative prediction for units from supplier B. The mean values of V_{obs}/V_{pre} were below unity for every method when applied to the units from supplier A, while the mean values of V_{obs}/V_{pre} were above unity for every method except for ACI 318-05 when applied to those from supplier B.

The most striking observation from Fig. 11 and 12 is the different performance of the various design formulas when applied to units from two different manufacturers. Three important questions are evident:

- Why is there such a disparity among the different shear-strength-prediction methods?
- Why is there such a disparity in the performance of the units from the two suppliers?
- Which method is most applicable to the shear design of hollow-core units?

Table 3. Parameters for hollow-core units from suppliers A and B

Supplier	Parameter	Shear prediction method				
		ACI 318-05	Eurocode 2	Yang	MCFT	AASHTO
A	b_w , in.	16.17	16.17	17.19	16.17	16.17
	f_{pc} , ksi	152	155	100	100	171
	f'_c , psi	6000	6000	6000	6000	6000
	f_{ct} , psi	271*	316	310 [†]	310 [†]	n.d. [‡]
	L_t , in.	25	23.6	25	25	30
	x_{cr} , in.	8	8	4.5	4.5 [§]	13.5
B	b_w , in.	11.73	11.73	12.1	11.73	11.73
	f_{pc} , ksi	407	582	249	249	380
	f'_c , psi	9826	9826	9826	9826	9826
	f_{ct} , psi	343 [*]	441	396 [†]	396 [†]	n.d. [‡]
	L_t , in.	26.7	17.7	26.7	26.7	32.4
	x_{cr} , in.	8	8	3.74	3.74 [‡]	11.5

* $3.5 \sqrt{f'_c}$, tensile strength implied by ACI 318-05 Eq. (11-12)

[†] $4 \sqrt{f'_c}$

[‡] Not calculated explicitly

[§] Assumed location for calculation of f_{pc} for computer program input

Note: AASHTO = American Association of State Highway and Transportation Officials; b_w = web width; f'_c = specified compressive strength of concrete; f_{ct} = tensile strength of concrete; f_{pc} = compressive stress in concrete at centroid of cross section resisting externally applied loads after allowance for all prestress losses; L_t = transfer length of prestressing strand; MCFT = modified compression field theory; n.d. = no data; x_{cr} = distance from center of support to critical point. 1 in. = 25.4 mm; 1 psi = 6.895 kPa; 1 ksi = 6.895 MPa.

Possible answers to these questions follow.

Disparity among shear-design (prediction) methods

To answer the first question, we compared relevant parameters for both suppliers. **Table 3** lists these parameters for the hollow-core units from suppliers A and B. Because Yang’s method and the modified compression field theory are not codified, the values of some of the parameters were chosen to match ACI 318-05 provisions. In the case of modified compression field theory, the prestressing force in the section was chosen as that coinciding with Yang’s critical location. The choice of parameters affects the predictions, but a complete study of the parameters for Yang’s method and the modified compression field theory was not done.

From Table 3, the values of some of the parameters for supplier A varied among methods. The value of f_{pc} per Yang’s method was 33% less than that of ACI 318-05 and Eurocode 2, while the value for AASHTO LRFD specifications was 13% higher than that for ACI 318-05. The lower value of f_{pc} for Yang’s method is a direct result of the critical point being located closer to the support than it

was for ACI 318-05, AASHTO LRFD specifications, and Eurocode 2.

The tensile strength as calculated according to Eurocode 2 was 17% larger than that implied by ACI 318-05, while the rest of the parameters shown in the table are similar between the two methods. Eurocode 2’s shear strength is slightly more conservative than the ACI 318-05 tensile strength due to the cross-section parameters. Namely, the ratio V/Q in Eurocode 2, which appears because of the parabolic shear stress distribution, is 80% of the value of d_p , which ACI 318-05 uses based on a constant average shear stress. Yang’s method provides a more conservative estimate for three reasons: a smaller prestressing force at the critical point, the use of the parabolic shear stress distribution, and the fact that the critical point is not at the centroid.

The influences of the parameters on the modified compression field theory and AASHTO LRFD specifications are not as easily extracted because of their formulations, but it can be argued that these provide better predictions than ACI 318-05 because they represent the mechanics of the problem more accurately. Namely, all sectional forces and

the effect of the longitudinal strain on the shear strength are considered. The value of f_{pc} per AASHTO LRFD specifications was greater than f_{pc} per all of the other methods, yet AASHTO LRFD specifications still provided the best prediction for supplier A.

Table 3 also shows the values of the parameters for supplier B. Again the parameters varied among methods. There was a large difference between ACI 318-05's and Eurocode 2's values for f_{pc} , f_{ct} , and L_t . The transfer length per ACI 318-05 was 9 in. (229 mm) longer than that calculated per Eurocode 2, which results in f_{pc} being 43% larger. In addition, f_{ct} per Eurocode 2 was 29% larger than f_{ct} calculated by ACI 318-05. These factors account for the large differences in V_{obs}/V_{pre} between ACI 318-5 and Eurocode 2 for supplier B. The observations made for the other methods for supplier A also applied to supplier B.

Unlike in ACI 318-05, the tensile strength of the concrete is considered in the Eurocode 2 transfer-length expression. Although the tensile strength has been shown to affect the transfer length,^{24,25} it is unclear whether this effect is accurately represented in this case because extensive transfer-length experiments on hollow-core units have not been conducted.

Disparity between manufacturers The second question regarding the disparity of the V_{obs}/V_{pre} between suppliers has not been adequately resolved to date. The authors investigated the possibility that this disparity was caused by uneven web-shear distribution combined with the differing shear strengths of the individual webs. Finite-element analyses were performed on the units from both suppliers to determine the web-shear distribution. Units from supplier A were found to have a highly uneven distribution of shear in the individual webs, while units from supplier B had a more uniform web-shear distribution (see the section "Transverse Distribution Effect").

Shear-capacity predictions of units from both suppliers were made based on the web-shear distribution found in the finite-element analysis and the capacities of the individual webs based on the prestressing occurring only in each respective web. The latter was based on the assumption that due to the shear lag across the width at the critical point where the strands have not been fully developed, the prestress experienced by the individual webs was only due to the strands in each respective web. Accordingly, units from supplier A, for which the webs had debonded strands, were assumed to have no prestress at all. All of the prediction methods used in the section "Comparison of U.S. Manufacturer Tests to Various Shear Prediction Methods" were used in the analysis described next. The analysis method was as follows:

1. Determine which webs would fail first based on their capacity and the web-shear distribution.

2. Determine if the remaining webs have enough capacity to absorb the load from the webs that theoretically fail first. If they can, determine which webs would fail next.
3. Once the remaining webs could no longer sustain the additional load, calculate the total shear based on the shear in the failed webs and the distribution of shear to the individual webs.

Figures 13 and 14 show V_{obs}/V_{pre} plotted against V_{pre} for the above analysis. When the web-shear distribution based on the finite-element analysis was taken into account, the shear predictions became more conservative for both suppliers' units. For the units from supplier A, all were greater than unity for the AASHTO LRFD specifications and Yang methods, while the other three methods generated shear-strength predictions that were below unity for all of the units. ACI 318-05 still provided the most unconservative predictions. For units from supplier B, all methods except ACI 318-05 and Eurocode 2 provided conservative predictions for all of the units.

If the cause of the disparity between the two suppliers was the uneven distribution of shear stress in the cross section, as well as the differing shear strengths of individual webs, then the predicted shear strengths for the units from supplier B should indicate a similarity in results from the two analyses' procedures. This would follow from the near-uniform distribution of shear stresses across the section obtained from the finite-element analysis (Fig. 10). However, this was not the case. The predicted shear strengths based on the finite-element distribution, relative to the predictions ignoring this effect, followed trends similar to those of the predictions for the units from supplier A. This indicates that the finite-element analysis may not accurately reflect the actual web-shear distribution and/or the approximation of shear strength because the sum of the individual web-shear strengths is not an accurate assumption.

Another possibility for the disparity between suppliers is that the actual tensile strengths of the concrete in the webs of the units from supplier A were not adequately represented by the prediction methods considered in this study. It would also follow that the concrete tensile strength for the units from supplier B are more adequately represented by the prediction formulas. Tensile strength will also have an impact on the transfer length of the strands for each supplier. Both of these conjectures, along with the web-shear distribution, need to be determined experimentally.

Best method for shear design of hollow-core units The most applicable method for shear prediction in the design of hollow-core units should include all of the relevant parameters and be capable of predicting the shear capacity in a consistently accurate and conservative man-

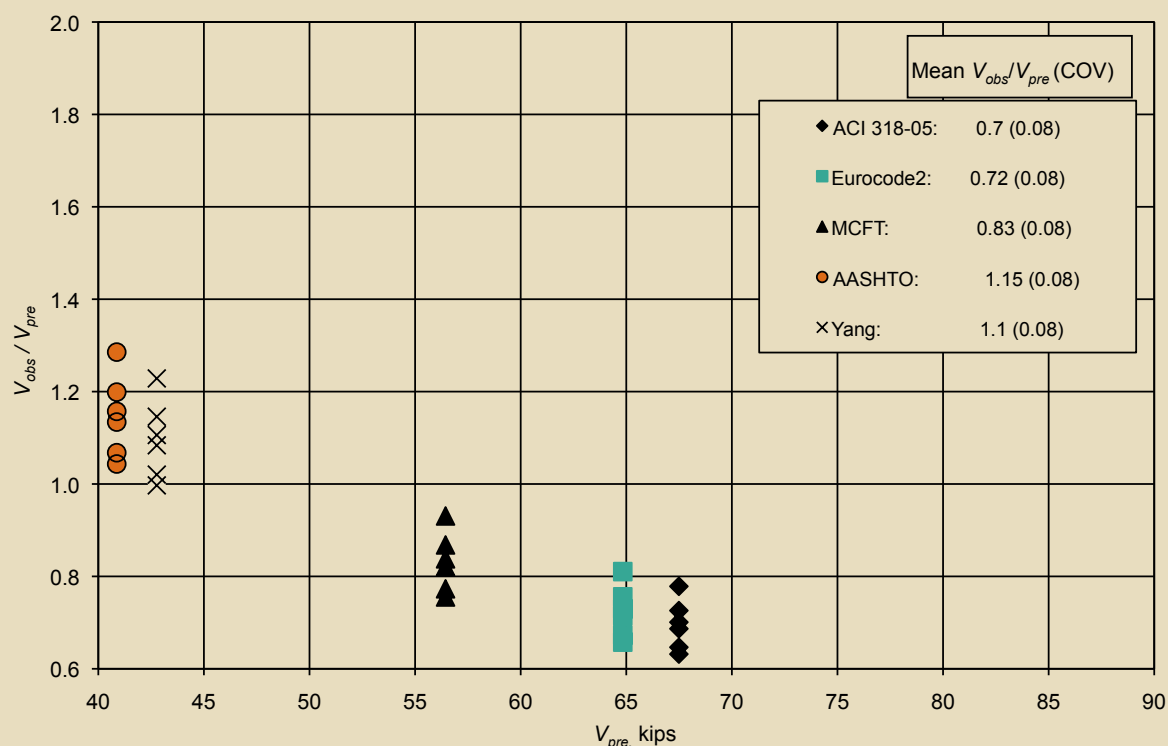


Figure 13. This graph shows V_{obs}/V_{pre} for supplier A's units based on finite-element web-shear distribution and individual web capacities. Note: AASHTO = American Association of State and Highway Transportation Officials; COV = coefficient of variation; MCFT = modified compression field theory; V_{obs}/V_{pre} = ratio of observed-to-predicted shear strengths; V_{pre} = predicted shear strength. 1 kip = 4.448 kN.

ner. The method increases in complexity as more parameters are added to the formulation. However, a rational formula that is to be used in design must balance the complexity of the procedure with accuracy and conservatism.

The procedure outlined in ACI 318-05 is the simplest method of those that are included in this study, but it also provided the most unconservative prediction for the units from supplier A and the second-most-unconservative prediction for the units from supplier B. The most complex method, the modified compression field theory, provided a good prediction for the units from supplier B and a poor prediction for those from supplier A. Yang's method, which is more complex than the ACI 318-05 and Eurocode 2 formulations, and arguably more complex than AASHTO LRFD specifications due to the large number of section properties that need to be calculated, provided a conservative prediction for all units from supplier B but an unconservative prediction for those from supplier A.

ACI 318-05 Eq. (11-12) is not applicable in its present form for the 16-in.-thick (410 mm) hollow-core-unit tests reported in this study from two U.S. manufacturers. A simple multiplicative reduction factor (that is, a constant coefficient less than unity), based on experimental results, could be applied to ACI 318-05 Eq. (11-12), and this has, in fact, been done in ACI 318-08. However, considering the variation of shear strengths between manufacturers, a general reduction based

on the worst case unduly penalizes units that displayed a more satisfactory performance. In addition, this reduction is not based on a logical and rational approach that addresses the underlying reasons behind the unconservativeness of the ACI 318-05 web-shear equation.

Yang's equation is applicable to the units from supplier B and to those from supplier A if the web-shear distribution and variation in individual web capacities are considered. However, the use of that latter correction is dubious given that it decreases the accuracy of the predicted shear strengths for the units from supplier B. In practice, the complexity of Yang's equation is noted here as being less severe than Eq. (4) suggests because all of the section properties required for this equation are constant for a given type of hollow-core-unit cross section. Under such circumstances, only four variables may change in Yang's equation for a given cross section. These variables are strand eccentricity, concrete tensile strength, prestressing force, and prestressing-force gradient. Yang's equation is advantageous because it is based on a mechanics-of-materials formulation, and it includes the effects of the prestressing-force gradient on shear stresses as well as the effect of the void geometry on the location of the maximum principal tensile stresses.

The modified compression field theory procedure appears applicable to the units from supplier B, but it yielded unconservative

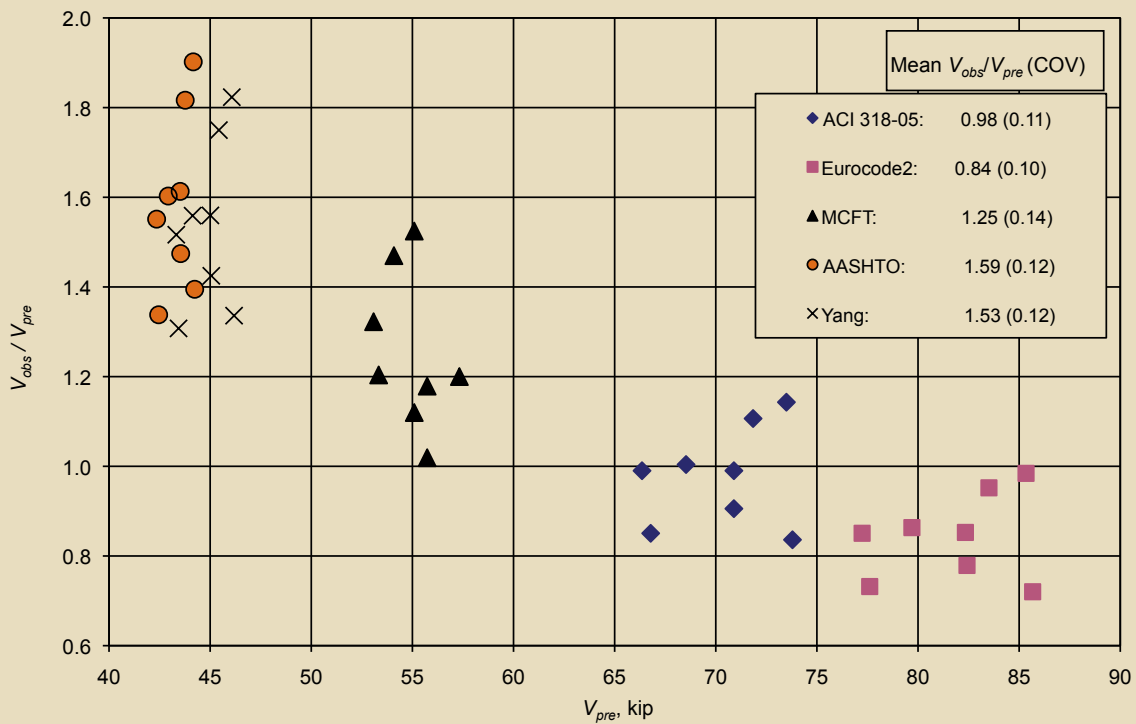


Figure 14. This graph shows V_{obs}/V_{pre} for supplier B's units based on finite-element web-shear distribution and individual web capacities. Note: AASHTO = American Association of State and Highway Transportation Officials; COV = coefficient of variation; MCFT = modified compression field theory; V_{obs}/V_{pre} = ratio of observed-to-predicted shear strengths; V_{pre} = predicted shear strength. 1 kip = 4.448 kN.

vative predictions for those from supplier A. Given the complexity of the method, it is cumbersome for use in the typical calculations needed for the design of hollow-core units.

The AASHTO LRFD specifications method provided good shear-strength predictions for the units from supplier B and the best predictions for those from supplier A. Even so, the predictions were found to be unconservative for all of the units from supplier A but one. The AASHTO LRFD specifications method is more intensive computationally than the ACI 318-05 or Eurocode 2 formulas because it is an iterative procedure but is easily programmed into a spreadsheet. It is a simpler design procedure and thus more viable than the modified compression field theory procedure from which it was derived.

Overall, the AASHTO LRFD specifications method appears to be best suited for shear design of hollow-core units. However, this question cannot be fully resolved until a rational explanation is found for the mechanism that produced the reported differences in the performance of the shear-strength-prediction methods for the units from the two suppliers.

Conclusion

The analytical work summarized in this paper on the web-shear strength of deep hollow-core units was undertaken

due to concerns from the industry that ACI 318-05 Eq. (11-12) provided unconservative shear-capacity predictions. This fact was borne out in shear tests undertaken by two U.S. manufacturers of hollow-core units. Units from supplier A failed at 61% of the values predicted by ACI 318-05 Eq. (11-12), and supplier B units failed at 91% of the values from ACI 318-05 Eq. (11-12). The relevant parameters affecting the web-shear capacity of hollow-core units were discussed, and a comparison was made between the observed experimental shear capacities and the capacities predicted by five different methods. Based on these analyses, the following conclusions were made:

- Analysis of 198 hollow-core units failing in shear found in the literature revealed that there is no clear evidence of a size effect in shear for units up to 19.7 in. (500 mm) in depth, due in part to the large scatter of the web-shear-strength data.
- There is a possibility that the tensile strength of the web concrete varies between the units from the two manufacturers that were considered in this study, and this may be the reason for the disparity in performance between the suppliers. More experimental research needs to be undertaken to assess this possibility.
- The geometry of the cross section can have an impact on the shear capacity of these units. Yang demon-

strated how void geometry affects the location of the maximum principal tensile stresses, moving the critical point lower in the section and closer to the support than is assumed by ACI 318-08 and ACI 318-05, AASHTO LRFD specifications, and Eurocode 2.

- Theoretically, the relative stiffness of the individual webs may affect the distribution of shear across the section. This, coupled with the shear lag of the prestressing force across the width, may tend to further reduce the shear capacity of hollow-core units. While this is theoretically possible, the comparisons between the two suppliers based on that analysis indicate that this is not the likely cause of the disparity between them.
- An accurate estimate of the prestressing force at the critical point requires an accurate estimate of the transfer length and transfer-stress distribution of the strands. It is unclear at this point whether a transfer length of $50d_b$, as recommended by ACI 318-08 and ACI 318-05 is applicable to extruded hollow-core units because no transfer-length experiments of U.S. manufactured units have been reported.
- Given the disparity in predicted shear capacities of the units from suppliers A and B, none of the prediction methods considered in this study were able to provide uniform reliability in shear-strength prediction. However, the AASHTO LRFD specifications method, followed by Yang's method, performed better than ACI 318-05, Eurocode 2, and the modified compression field theory.
- More research is needed to resolve the question regarding the most applicable shear-prediction method for deep hollow-core units and to develop a more rational and logical revision than an overall reduction factor to the web-shear predictions based on ACI 318-05. Specifically, experiments should be undertaken for the following reasons:
 - to increase the number of shear-capacity tests conducted on thick hollow-core units
 - to determine the variation, if any, of the concrete tensile strength as a function of the compressive strength across a range of U.S. manufacturers
 - to determine the strand transfer length and the shape of the prestressing-force gradient across a range of U.S. manufacturers
 - to verify the finite-element-analysis results that indicate an uneven web-shear distribution

To address providing uniform reliability in shear-strength prediction, an experimental program is ongoing at the University of Minnesota. The program includes web-shear failure tests of hollow-core units, provided by two U.S. manufacturers, with depths equal to 12 in., 16 in., and 20 in. (300 mm, 410 mm, and 510 mm). Instrumentation of the units will serve to verify the observations regarding web-shear stress distributions from the finite-element analyses. Tests are also being conducted to determine the strand transfer length and prestressing-force gradient. The method used for the transfer-length tests is similar to that used by Walraven and Mercx.

Acknowledgments

This work was supported in part by PCI through a Daniel P. Jenny Fellowship and by the Department of Civil Engineering at the University of Minnesota through a Sommerfeld Fellowship awarded to Keith D. Palmer. Special thanks go to Paul Kourajian for his help and technical advice throughout this project.

References

1. Buettner, Donald R., and Roger J. Becker. 1998. *PCI Manual for the Design of Hollow Core Slabs*. 2nd ed. Chicago, IL: PCI.
2. Hawkins, Neil M., and S. K. Ghosh. 2006. Shear Strength of Hollow-Core Slabs. *PCI Journal*, V. 51, No. 1 (January–February): pp. 110–115.
3. American Concrete Institute (ACI) Committee 318. 2008. *Building Code Requirements for Structural Concrete (ACI 318-08) and Commentary (ACI 318R-08)*. Farmington Hills, MI: ACI.
4. Kani, G. N. J. 1967. How Safe Are Our Large Concrete Beams? *Journal of the American Concrete Institute*, V. 64, No. 3 (March): pp. 128–141.
5. Collins, Michael P., and Daniel Kuchma. 1999. How Safe Are Our Large, Lightly Reinforced Concrete Beams, Slabs, and Footings? *ACI Structural Journal*, V. 96, No. 4 (July–August): pp. 482–490.
6. Bazant, Zdenek P., and Mohammad T. Kazemi. 1991. Size Effect on Diagonal Shear Failure of Beams without Stirrups. *ACI Structural Journal*, V. 88, No. 3 (May–June): pp. 268–276.
7. Angelakos, Dino, Evan C. Bentz, and Michael P. Collins. 2001. Effect of Concrete Strength and Minimum Stirrups on Shear Strength of Large Members. *ACI Structural Journal*, V. 98, No. 3 (May–June): pp. 290–300.

8. ACI Committee 318. 2005. *Building Code Requirements for Structural Concrete (ACI 318-05) and Commentary (ACI 318R-05)*. Farmington Hills, MI: ACI.
9. Pajari, Matti. 2005. Resistance of Prestressed Hollow-Core Slabs against Web Shear Failure. *Research Notes 2292*, p. 62. Kemistintie, Finland: VTT Building and Transport.
10. Yang, Lin. 1994. Design of Prestressed Hollow-Core Slabs with Reference to Web Shear Failure. *Journal of Structural Engineering*, V. 120, No. 9 (September): pp. 2675–2696.
11. EN 1992-1-1. 2004. *Eurocode No. 2: Design of Concrete Structures-Part 1: General Rules and Rules for Buildings*. Brussels, Belgium: The Commission of the European Communities.
12. Vecchio, Frank J., and Michael P. Collins. 1986. The Modified Compression-Field Theory for Reinforced Concrete Elements Subjected to Shear. *Journal of the American Concrete Institute*, V. 83, No. 2 (March–April): pp. 219–231.
13. Vecchio, F. J., and M. P. Collins. 1988. Predicting the Response of Reinforced Concrete Beams Subjected to Shear Using Modified Compression Field Theory. *ACI Structural Journal*, V. 85, No. 3 (May–June): pp. 258–268.
14. American Association of State Highway and Transportation Officials (AASHTO). 2004. *LRFD Bridge Design Specifications*. 3rd ed. Washington, DC: AASHTO.
15. Walraven, J. C., and W. P. M. Mercx. 1983. The Bearing Capacity of Prestressed Hollow-Core Slabs. *HERON*, V. 28, No. 3: pp. 1–46.
16. Olsen, D. H., C. Ganwei, and M. P. Nielsen. 1990. Plastic Shear Solutions of Prestressed Hollow-Core Concrete Slabs. *Afdelingen for Baerende Konstruktioner*, Series R, No. 257, Department of Structural Engineering, Technical University of Denmark, Lyngby.
17. Becker, Roger J., and Donald R. Buettner. 1985. Shear Tests of Extruded Hollow-Core Slabs. *PCI Journal*, V. 30, No. 2 (March–April): pp. 40–54.
18. Pisanty, A. 1992. The Shear Strength of Extruded Hollow-Core Slabs. *Materials and Structures*, No. 25 (May): pp. 224–230.
19. Bentz, Evan C. 2005. Empirical Modeling of Reinforced Concrete Shear Strength Size Effect for Members without Stirrups. *ACI Structural Journal*, V. 102, No. 2 (March–April): pp. 232–241.
20. Jonnson, Esben. 1988. Shear Capacity of Prestressed Extruded Hollow-Core Slabs. *Nordic Concrete Research*, No. 7: pp. 167–187.
21. Nilson, Arthur H. 1987. *Design of Prestressed Concrete*. 2nd ed. New York, NY: John Wiley and Sons.
22. Cousins, Thomas E., David W. Johnston, and Paul Zia. 1990. Transfer and Development Length of Epoxy-Coated and Uncoated Prestressing Strand. *PCI Journal*, V. 35, No. 4 (July–August): pp. 92–103.
23. Rose, Dallas R., and Bruce W. Russell. 1997. Investigation of Standardized Tests to Measure the Bond Performance of Prestressing Strand. *PCI Journal*, V. 42, No. 4 (July–August): pp. 56–80.
24. Barnes, Robert W., John W. Grove, and Ned H. Burns. 2003. Experimental Assessment of Factors Affecting Transfer Length. *ACI Structural Journal*, V. 100, No. 6 (November–December): pp. 740–748.
25. Oh, Byung Hwan, and Eui Sung Kim. 2000. Realistic Evaluation of Transfer Lengths in Pretensioned, Prestressed Concrete Members. *ACI Structural Journal*, V. 97, No. 6 (November–December): pp. 821–830.
26. Abrishami, Homayoun H., and Denis Mitchell. 1933. Bond Characteristics of Pretensioned Strand. *ACI Materials Journal*, V. 90, No. 3 (May–June): pp. 228–235.
27. Kose, M. M., and W. R. Burkett. 2005. Evaluation of Code Requirement for 0.6 in. (15 mm) Prestressing Strand. *ACI Structural Journal*, V. 102, No. 3 (May–June): pp. 422–428.
28. Martin, Leslie D., and Norman L. Scott. 1976. Development of Prestressing Strand in Pretensioned Members. *ACI Journal*, V. 73, No. 8 (August): pp. 453–456.
29. Shahawy, Mohsen A., Moussa Issa, and Barrington deV. Batchelor. 1992. Strand Transfer Lengths in Full Scale AASHTO Prestressed Concrete Girders. *PCI Journal*, V. 37, No. 3 (May–June): pp. 84–96.
30. Tabatabai, Habib, and Timothy J. Dickson. 1993. The History of the Prestressing Strand Development Length Equation. *PCI Journal*, V. 38, No. 6 (November–December): pp. 64–75.
31. Brooks, Mark D., Kurt H. Gerstle, and Donald R. Logan. 1988. Effect of Initial Strand Slip on the Strength

of Hollow-Core Slabs. *PCI Journal*, V. 33, No. 1 (January–February): pp. 90–111.

32. Mitchell, Denis, William D. Cook, Arshad A. Khan, and Thomas Tham. 1993. Influence of High Strength Concrete on Transfer and Development Length of Prestensioning Strand. *PCI Journal*, V. 38, No. 3 (May–June): pp. 52–66.
33. Russell, Bruce W., and Ned H. Burns. 1996. Measured Transfer Lengths of 0.5 and 0.6 in. Strands in Prestensioned Concrete. *PCI Journal*, V. 41, No. 5 (September–October): pp. 44–63.
34. Tasuji, M. Ebrahim, Floyd O. Slate, and Arthur H. Nilson. 1978. Stress-Strain Response and Fracture of Concrete in Biaxial Loading. *Journal of the American Concrete Institute*, V. 75, No. 7 (July): pp. 306–312.
35. Kupfer, Helmut, Hubert K. Hilsdorf, and Hubert Rusch. 1969. Behavior of Concrete under Biaxial Stresses. *Journal of the American Concrete Institute*, V. 66, No. 8 (August): pp. 656–666.
36. Hussein, A., and H. Marzouk. 2000. Behavior of High-Strength Concrete under Biaxial Stresses. *ACI Materials Journal*, V. 97, No.1 (January–February): pp. 27–36.
37. ACI-ASCE Committee 326. 1962. Shear and Diagonal Tension, pt. 2. *Journal of the American Concrete Institute*, V. 59, No. 2 (March): pp. 277–334.
38. Neville, Adam M. 1996. *Properties of Concrete*. New York, NY: John Wiley and Sons Inc.
39. Pisanty, A., and P. E. Regan. 1991. Direct Assessment of the Tensile Strength of the Web in Prestressed Precast Hollow-Core Slabs. *Materials and Structures*, V. 24, No. 6 (November): pp. 451–455.
40. MacGregor, James G. 1997. *Reinforced Concrete, Mechanics and Design*. 3rd ed. Upper Saddle River, NJ: Prentice Hall.
41. Hawkins, Neil M., Daniel A. Kuchma, Robert F. Mast, M. Lee Marsh, and Karl-Heinz Reineck. 2005. Simplified Shear Design of Structural Concrete Members. NCHRP report 549. Washington, DC: Transportation Research Board.
42. Bentz, Evan C. 2000. Sectional Analysis of Reinforced Concrete. PhD thesis. Department of Civil Engineering, University of Toronto.
43. Bentz, Evan C. Response 2000. www.ecf.utoronto.ca/~bentz/home.shtml.

Notation

a	= shear span
A_{cp}	= area of section above the critical point
A_g	= gross area of concrete section, excluding voids
b_w	= web width
COV	= coefficient of variation
d	= distance from extreme compression fiber to centroid of longitudinal reinforcement
d_b	= nominal diameter of prestressing strand
d_p	= distance from extreme compression fiber to centroid of prestressing steel
e	= eccentricity of strand measured from the centroid
f'_c	= specified compressive strength of concrete
f_{ct}	= tensile strength of concrete
f_{ctd}	= design tensile strength of concrete
f_{pc}	= compressive stress in concrete at centroid of cross section resisting externally applied loads after allowance for all prestress losses
f_{se}	= effective stress in prestressing steel after allowance for all prestress losses
h	= overall thickness or height of member
I	= moment of inertia of section about centroidal axis
L	= overall span of unit in manufacturer tests
L_t	= transfer length of prestressing strand
N_p	= prestressing force in strand
Q	= first area moment of section about centroidal axis
S_{cp}	= first area moment of section about critical-point axis
v	= shear stress
V	= shear in section

V_c	= nominal shear resistance of concrete
V_{cw}	= nominal web-shear cracking strength
V_n	= nominal shear strength
V_{obs}	= experimentally observed failure shear at critical point
V_p	= vertical component of effective prestressing force at critical section
V_{pre}	= predicted shear strength
$V_{Rd,c}$	= predicted web-shear cracking strength
V_s	= nominal shear resistance of transverse reinforcement
V_{yang}	= predicted web-shear strength
x_{cp}	= distance from center of support to critical point (notation according to Yang)
x_{cr}	= distance from center of support to critical point
z_{cp}	= vertical distance from centroid to critical point
α_l	= ratio of distance from end of member to transfer length
β	= factor indicating ability of diagonally cracked concrete to transmit tension
$\partial N_p / \partial x$	= prestressing-force gradient
σ_{cp}	= fully effective concrete compressive stress at the centroid due to prestressing

About the authors



Keith D. Palmer, P.E., is a graduate research assistant for the Department of Civil Engineering at the University of Minnesota, Twin Cities Campus, in Minneapolis.



Arturo E. Schultz, PhD, is a professor for the Department of Civil Engineering at the University of Minnesota, Twin Cities Campus.

Synopsis

Shear-strength estimates for precast, prestressed hollow-core units in the United States follow the shear recommendations of the American Concrete Institute's (ACI's) Committee 318. These recommendations are based on experimental research done mainly on members other than hollow-core units, and they have been extended to hollow-core units based on a limited amount of hollow-core shear tests.

Recent shear tests that several U.S. manufacturers have performed on thick hollow-core units (units with depths larger than 12 in. [300 mm]) have indicated failures in the web at forces smaller than those predicted by *Building Code Requirements for Structural Concrete (ACI 318-05)* and *Commentary (ACI 318R-05)*. Similar observations have been made by researchers in Europe, where web-shear provisions are similar in nature to those in ACI 318-05.

As a stopgap measure, ACI 318-08 waives the exception on minimum shear reinforcement for hollow-core units deeper than 12.5 in. (318 mm). An analytical research program at the University of Minnesota investigated the reasons that thicker hollow-core units fail at lower shear forces than those predicted using the ACI 318-05 provisions. This paper summarizes the findings of the analytical program, including comparisons of the ACI 318-05, *Eurocode No. 2: Design of Concrete Structures-Part 1: General Rules and Rules for Buildings*, the modified compression field theory, the American Association of State Highway and Transportation Officials' *AASHTO LRFD Bridge Design Specifications*, and Yang's shear prediction methods.

Keywords

Design formula, hollow-core, shear test, size effect, tensile strength, transfer length, web-shear strength.

Review policy

This paper was reviewed in accordance with the Precast/Prestressed Concrete Institute's peer-review process.

Reader comments

Please address any reader comments to *PCI Journal* editor-in-chief Emily Lorenz at elorenz@pci.org or Precast/Prestressed Concrete Institute, c/o *PCI Journal*, 200 W. Adams Street, Suite 2100, Chicago, IL 60606. 